Motion Characteristic Analysis of a Hybrid-Driven Underwater Glider

S. X. Wang, X. J. Sun, J. G. Wu, X. M. Wang, H. W. Zhang
School of Mechanical Engineering, Tianjin University
92 Weijin Road, Nankai District
Tianjin 300072 China

***Abstract*- PETREL, a winged hybrid-driven underwater glider is presented, which features long-endurance low-noise while penetrating the ocean like a UW glider and burst-speed high-maneuverability while operated as an AUV. In addition, kinematic and dynamic model of the vehicle are developed based the theorem of momentum and moment of momentum. Moreover, equations of equilibrium indicating the balance pitch and attack angles are deduced and indexes for evaluation of maneuverability of this vehicle in 6-DOF are defined. Furthermore, its specific characters are investigated by simulation and the functionality is validated by field trial. In thrust operation, the external bladder for buoyancy change improves the efficiency of pitch control while mounted on the fore end of vehicle and the swerving radius is largely decreased by using vertical fins for steering instead of roll mass; Meanwhile in glide operation, the longitudinal maneuverability is largely increased due to the fixed wings and the capability of attitude keeping is augmented by redistribution of internal mass (roll and pitch mass) while the vehicle cruises at low speed.**

I. INTRODUCTION

Conventional AUVs and legacy underwater gliders have played more and more important role in oceanographic survey recently [1, 2]. Underwater gliders roam the ocean in dolphin glide path stealthily with low power consumption, long duration, and the capability of station keeping. However, their low degree of maneuverability make it difficult to follow the prescribed trajectory exactly, their low speed make it impossible to penetrate the large scale ocean circulation and coastal currents, and their transport economy is largely decreased while they cruise in littoral and estuary waters due to the shallow depth. Conventional AUVs are operated underwater with high maneuverability due to the mounted powerful thrust system. However, their cross country capability seems to be pale before the legacy gliders due to their inferior efficiency of energy consumption, and the capability of attitude keeping with large roll or pitch angle does not work well when the rudder-steering class vehicles navigate at low speed.

In order to combine the advantages and overcome the disadvantages of the two types of underwater vehicles, PETREL, a winged hybrid-driven underwater glider has been designed and tested in Tianjin University, China [3]. Actually, for the purpose of multi-functionality, it is designed as a redundancy system actually by optimum integration of conventional AUVs and legacy gliders. The basic components such as roll mass, pitch mass and buoyancy bladder are inherited from legacy gliders such as Slocum, Spray, Seaglider [4-6], and the fundamental configuration of four cross-shaped rudders and single aft-mounted propeller are borrowed from conventional AUVs such as REMUS, Gavia and AUTOSUB etc [7-9].

Due to the best features of hybrid glider as described in the technical report “Underwater Glider System Study” by Scripps Institution of Oceanography, 2003, the hybrid glider has been developed for many years and several hybrid prototypes have been fabricated and tested [10]. A conceptual draw of hybrid glider was proposed by R. Bachmayer 2004, and it’ far away from the implementation [11]. AUV Powered Glider is illustrated in a report “Autonomous Underwater Vehicle: Powered Glider” by Todd Allen, Florida Institute of Technology in 2006. It can be propelled and veered by dual aft-mounted screws to perform thrust operation or be altered to glide operation through buoyancy driving and body-wing flapping [12]. SEAEXPORER is introduced in a presentation “Innovative Glider Technologies” by La Spezia, 2008, which performs hybrid-driven operation by replacing the nose dome with a thruster, especially there’s no moving components outside vehicle except for thruster. Folaga is a type of hybrid vehicle which combines the capabilities of gliders and AUVs, it dives into the ocean for measurement with the actuation of buoyancy, and changes its position by waterjet thrust [13]. Sterne is another hybrid one which is comprised of fixed wings, actuated horizontal tail fins, vertical tail rudder and powerful propeller [14]. There are two types of operations for the hybrid glider: one is thrust mode in which the vehicle is propelled forward with thruster, and the other is glide mode in which the vehicle is driven by net buoyancy and pushed ahead with the hydrodynamic lift of body and wings. Although the emerged hybrid gliders performed both glide and thrust operations, the configurations are varied with each other.

Electric Slocum has been used as a hybrid prototype by fitting with an aft-mounted propeller to evaluate the performance of hybrid class vehicle. From the experiment photo of the Electric Slocum found in [15], its configuration is a little like PETREL, while its detailed description of system fabrication, and dynamic modeling for motion behavior evaluation were not be published yet. Combined with conventional AUVs and legacy gliders, PETREL is designed to be a typical hybrid glider. It possesses the common features of hybrid gliders and individuality unlike the other hybrids.

978-1-4244-5222-4/10/$26.00 ©2010 IEEE

II. Fabrication and Operation

PETREL is an optimal integration of a powered AUV built on a legacy glider base. In thrust mode the vehicle performs level flight with propeller propulsion and rudder steering, whereas in glide mode the vehicle penetrates the ocean in a dolphin glide path directed by ballast trimming and internal mass displacement (Fig.1). The dual propulsion architecture allows the single vehicle to maneuver optimally in a larger range of conditions than a standard AUV or underwater glider.

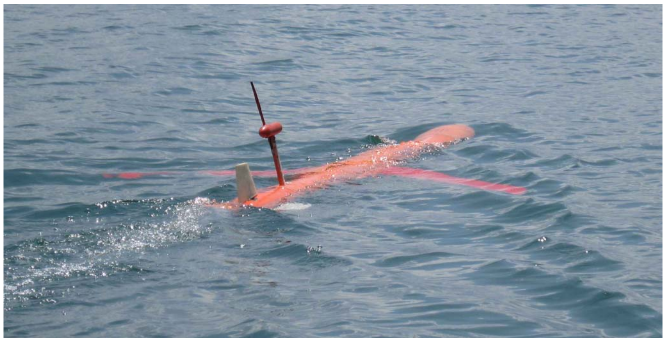

Figure 1. PETREL - a winged hybrid-driven underwater glider.

Thrust mode is switched on while cruising in shallow water region or burst speed and precise location is needed. Wherein, Rudder steering and prop driving modules get into work and roll regulating device cooperates to balance the roll moment generated by the rotating prop. Herein, the vehicle characterizes high maneuverability and high speed capability. Note that pitch adjusting and buoyancy actuating apparatuses are all reset to the neutral position in this mode.

Glide mode substitutes for the thrust mode while arriving at the deep-sea regime and requiring sounding the ocean environment through profiling and station maintenance. Then, roll and pitch regulator coordinates with buoyancy engine to travel in saw-tooth pattern like legacy gliders. Rudders can also substitute roll regulator for vehicle steering which is not considered in our present experiment. Here prop stops rotating and rudders are neutrally redisplayed. It features long-term, long-range, high efficiency and low noise ability in this mode.

The work modes are altered in terms of preprogrammed instruction or by command from remote control center while the vehicle is drifting at sea surface for data exchanging and GPS fix.

III. Dynamic Model of PETREL

The model of PETREL can be considered as few-body system, which is composed of roll mass m_r, pitch mass m_p and floating main mass m_h. The roll mass rotates about longitudinal axis of vehicle to balance the moment of propeller and change the roll attitude. The pitch mass translates along longitudinal axis to vary the pitch attitude. In order to facilitate the calculation of hydrodynamics, we consider the rudders and propeller as well as the floating main mass as a whole, i.e. the floating main mass includes the rudders and propeller. Mass change of external bladder is relatively small comparing with roll, pitch and main mass, so we can neglect the mass of external bladder and just define net buoyancy acting on the center of bladder. The buoyancy center is fixed on the shape center of the displaced water, and the mass center of PETREL is changeable. By assuming the relative motion of roll, pitch mass with the floating main mass to be at low and uniform speed, the generalized velocity of the three masses is considered to be the same.

As the first attempt to model the hybrid class vehicle, the theorem of momentum and moment of momentum used in the dynamic analysis of conventional AUVs are borrowed through tailored modification. The fundamental concepts and definitions such as transformation matrix, reference frames, generalized velocity, generalized position, hydrodynamic coefficients etc can be found in [16].

As shown in Fig. 3, the earth-fixed frame of reference and the body-fixed frame of reference are defined to facilitate the analysis of motion model. we define the force $\mathbf{F}_G=[X\ Y\ Z]^T$, the torque $\mathbf{M}_B=[K\ M\ N]^T$, the velocity $\mathbf{V}_B=[u\ v\ w]^T$, the angular rate $\mathbf{\Omega}=[p\ q\ r]^T$, the gravity center vector $\mathbf{R}_G=[x_G\ y_G\ z_G]^T$ with respect to body-fixed frame of reference. In addition, we define the moment of inertia about gravity center of vehicle as $\mathbf{J}_G=[J_{xG}\ J_{yG}\ J_{zG}]^T$ and the moment of inertia about the buoyancy center as $\mathbf{J}_B=[J_x\ J_y\ J_z]^T$.

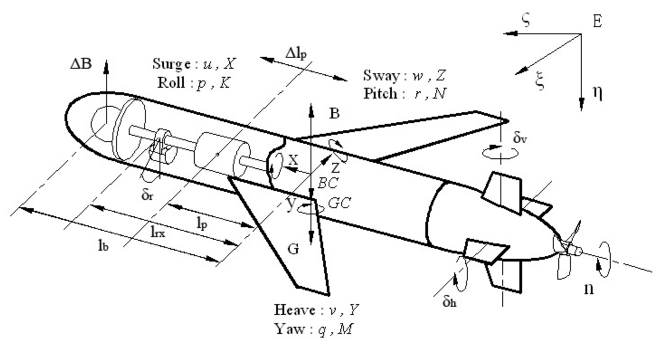

Figure 2. Frames of reference, state variables and control quantum.

According to momentum theorem, we have

$$m\dot{\mathbf{V}}_G = \mathbf{F}_G \tag{1}$$

where

$$\dot{\mathbf{V}}_G = \dot{\mathbf{V}}_B + \mathbf{\Omega}\times\mathbf{V}_B + \dot{\mathbf{\Omega}}\times\mathbf{R}_G + \mathbf{\Omega}\times\left(\mathbf{\Omega}\times\mathbf{R}_G\right)$$

and $\mathbf{F}_G$ is the resultant external force acting on gravity center and can be expressed as

$$\mathbf{F}_G = \mathbf{T}_E^B \cdot {}^E\mathbf{\Delta B} + \mathbf{T}_E^B \cdot {}^E\mathbf{B} + \mathbf{T}_E^B \cdot {}^E\mathbf{G} + \mathbf{F}_T + \mathbf{F}_H \tag{2}$$

where ${}^E\mathbf{\Delta B}$, ${}^E\mathbf{B}$ and ${}^E\mathbf{G}$ are respectively the net buoyancy, total buoyancy and total gravity expressed in earth-fixed frame. $\mathbf{F}_T$ is the force of thruster acting on vehicle. $\mathbf{T}_E^B$ is the transformation matrix from earth-fixed frame to body-fixed frame. The hydrodynamic force $\mathbf{F}_H$ is consisted of inertial and viscous components, viz.

$$\mathbf{F}_H = \mathbf{F}_{HV} + \mathbf{F}_{HI}$$

If we use $\mathbf{R}_r=[x_{Gr}\ y_{Gr}\ z_{Gr}]^T$, $\mathbf{R}_p=[x_{Gp}\ y_{Gp}\ z_{Gp}]^T$ and $\mathbf{R}_h=[x_{Gh}\ y_{Gh}\ z_{Gh}]^T$ to represent the vector of position of roll mass, pitch mass and main mass, then the vector of position of mass center of vehicle $\mathbf{R}_G$ in body frame can be depicted as

$$m\cdot\mathbf{R}_G = m_r\cdot\mathbf{R}_r + m_p\cdot\mathbf{R}_p + m_m\cdot\mathbf{R}_h \tag{3}$$

In light of the theorem of moment of momentum, we have

$$\dot{\mathbf{L}}_G = \mathbf{M}_G \tag{4}$$

where the moment of momentum $\mathbf{L}_G$ can be denoted as

$$\mathbf{L}_G = \mathbf{J}_G\cdot\mathbf{\Omega}^T$$
$$\dot{\mathbf{L}}_G = \mathbf{J}_G\cdot\dot{\mathbf{\Omega}}^T + \mathbf{\Omega}\times\mathbf{L}_G$$

and $\mathbf{M}_G$ denotes the resultant external torque acting on gravity center of vehicle, and can be expressed as

$$\mathbf{M}_G = \mathbf{M}_B - \mathbf{R}_G\times m\dot{\mathbf{V}}_G \tag{5}$$

$\mathbf{M}_B$, the external resultant torque acting on buoyancy center of vehicle is

$$\mathbf{M}_B = \mathbf{R}_b\times\mathbf{T}_E^B\cdot^E\Delta\mathbf{B} + \mathbf{R}_G\times\mathbf{T}_E^B\cdot^E\mathbf{G} + \mathbf{M}_T + \mathbf{M}_H$$

$\mathbf{M}_T$ denotes the hydrodynamic moment of propeller. $\mathbf{M}_H$, the hydrodynamic moment of body of vehicle is consisted of initial and viscous items, viz.

$$\mathbf{M}_H = \mathbf{M}_{HV} + \mathbf{M}_{HI}$$

Note that, $\mathbf{J}_G$ can be replaced with $\mathbf{J}_B$ by using the parallel axis theorem.

We denote the position of vehicle in earth-fixed frame of reference as $\mathbf{P}=[\xi_B\ \eta_B\ \zeta_B]^T$, and utilize the Cardan angles $\mathbf{A}=[\psi\ \theta\ \varphi]^T$ to express the attitude of vehicle. The kinematic equations of vehicle can be written as

$$\dot{\mathbf{P}} = \mathbf{T}_B^E\cdot\mathbf{V}_B \tag{6}$$

$$\dot{\mathbf{A}} = \mathbf{C}_B^E\cdot\mathbf{\Omega} \tag{7}$$

$\mathbf{T}_B^E$ transforms the vectors from body-fixed frame of reference to earth-fixed frame of reference. $\mathbf{C}_B^E$ acts as transform matrix from body-fixed frame to Cardan angles.

According to [17], the vicious hydrodynamic force and moment are expressed as

$$\mathbf{F}_{HV} = \begin{bmatrix} \frac{1}{2}\rho V_B^2 S X_0' \\ \frac{1}{2}\rho V_B^2 S\left(Y_\alpha' + Y_r' r' + Y_{\delta h}'\delta_h\right) \\ \frac{1}{2}\rho V_B^2 S\left(Z_\beta'\beta + Z_p' p' + Z_q' q' + Z_{\delta v}'\delta_v\right) \end{bmatrix}$$

$$\mathbf{M}_{HV} = \begin{bmatrix} \frac{1}{2}\rho V_B^2 SL\left(K_\beta'\beta + K_p' p' + K_q' q' + + K_{\delta v}'\delta_v\right) \\ \frac{1}{2}\rho V_B^2 SL\left(M_\beta'\beta + M_p' p' + M_q' q' + M_{\delta v}'\delta_v\right) \\ \frac{1}{2}\rho V_B^2 SL\left(N_\alpha'\alpha + N_r' r' + N_{\delta h}'\delta_h\right) \end{bmatrix}$$

and the initial hydrodynamic force and moment can be written as

$$\mathbf{F}_{HI} = \begin{bmatrix} -\lambda_{11}\dot{u} \\ -\lambda_{22}\dot{v} - \lambda_{26}\dot{r} \\ -\lambda_{33}\dot{w} - \lambda_{35}\dot{q} \end{bmatrix},\ \mathbf{M}_{HI} = \begin{bmatrix} -\lambda_{44}\dot{p} \\ -\lambda_{35}\dot{w} - \lambda_{55}\dot{q} \\ -\lambda_{26}\dot{v} - \lambda_{66}\dot{r} \end{bmatrix}$$

and the hydrodynamic thrust and torque of propeller are expressed as

$$\mathbf{F}_T = \begin{bmatrix} X_n'\rho n^2 D^4 \\ 0 \\ 0 \end{bmatrix},\ \mathbf{M}_T = \begin{bmatrix} K_n'\rho n^2 D^5 \\ 0 \\ 0 \end{bmatrix}$$

where $\{X'_{(.)}\ \ Y'_{(.)}\ \ Z'_{(.)}\ \ K'_{(.)}\ \ M'_{(.)}\ \ N'_{(.)}\}$ are respectively the hydrodynamic coefficients. The other denotations can be found in [18].

The transformation matrixes $\mathbf{T}_E^B$, $\mathbf{T}_B^E$ and $\mathbf{C}_B^E$ can be written as

$$\mathbf{T}_E^B = \begin{bmatrix} c\theta c\psi & s\psi s\varphi - s\theta c\varphi c\psi & c\varphi s\psi + s\theta c\varphi c\psi \\ s\theta & \cos\theta\cos\varphi & -s\varphi c\theta \\ -c\theta s\psi & c\varphi s\psi s\theta + s\varphi c\psi & c\psi c\varphi - s\varphi s\theta s\psi \end{bmatrix}$$

$$\mathbf{T}_B^E = \begin{bmatrix} c\theta c\psi & s\theta & -c\theta s\psi \\ -s\theta c\varphi c\psi + s\psi s\varphi & c\theta c\varphi & s\theta s\psi\cos\varphi + c\psi s\varphi \\ s\theta c\psi s\varphi + c\varphi s\psi & -s\varphi c\theta & -s\theta s\psi s\varphi + c\varphi c\psi \end{bmatrix}$$

$$\mathbf{C}_B^E = \begin{bmatrix} 1 & 0 & \sin\theta \\ 0 & \sin\varphi & \cos\theta\cos\varphi \\ 0 & \cos\varphi & -\cos\theta\sin\varphi \end{bmatrix}$$

note that c and s represent the cos and sin.

By substituting the hydrodynamic forces and torques and the transformation matrixes into (6) and (7), the dynamic and kinematic equations can be derived as follows

$$
\begin{cases}
(m+\lambda_{11})\dot{u}+mz_G\dot{q}-my_G\dot{r}-mvr+mwq-mx_G\left(q^2+r^2\right)+my_Gpq+mz_Gpr \\
=\Delta B\sin\theta+G\sin\theta+B\sin\theta+X'_n\rho n^2D^4+\frac{1}{2}\rho V_B^2SX'_0 \\
(m+\lambda_{22})\dot{v}-mz_G\dot{p}+(mx_G+\lambda_{26})\dot{r}-mwp+mur-my_G\left(r^2+p^2\right)+mz_Gqr+mx_Gqp \\
=\Delta B\cos\theta\cos\varphi+G\cos\theta\cos\varphi+B\cos\theta\cos\varphi+\frac{1}{2}\rho V_B^2S(Y'_\alpha\alpha+Y'_rr'+Y'_{\delta h}\delta_h) \\
(m+\lambda_{33})\dot{w}+my_G\dot{p}-(mx_G+\lambda_{35})\dot{q}-muq+mvp-mz_G\left(p^2+q^2\right)+mx_Grp+my_Grq \\
=-\Delta B\cos\theta\sin\varphi-G\cos\theta\cos\varphi-B\cos\theta\cos\varphi+\frac{1}{2}\rho V_B^2S\left(Z'_\beta\beta+Z'_pp'+Z'_qq'+Z'_{\delta v}\delta_v\right) \\
(J_x+\lambda_{44})\dot{p}-J_{xz}\dot{r}-J_{xy}\dot{q}-mz_G\dot{v}+my_G\dot{w}+J_{yz}\left(r^2-q^2\right)+\left(J_z-J_y\right)qr+my_G(vp-uq)-mz_G(ur-wp)+J_{xy}pr-J_{xz}pq \\
=-Gz_G\cos\theta\cos\varphi-Gy_G\cos\theta\sin\varphi+K'_n\rho n^2D^5+\frac{1}{2}\rho V_B^2SL\left(K'_\beta\beta+K'_pp'+K'_qq'+K'_{\delta v}\delta_v\right) \\
\left(J_y+\lambda_{55}\right)\dot{q}-J_{xy}\dot{p}-J_{yz}\dot{r}+mz_G\dot{u}-(mx_G+\lambda_{35})\dot{w}+J_{zx}\left(p^2-r^2\right)+(J_x-J_z)rp+mz_G(wq-vr)-mx_G(vp-uq)-J_{xy}qr+J_{yz}qp \\
=\Delta Bl_b\cos\theta\sin\varphi+Gz_G\cos\theta\cos\varphi+Gx_G\cos\theta\sin\varphi+\frac{1}{2}\rho V_B^2SL\left(M'_\beta\beta+M'_pp'+M'_qq'+M'_{\delta v}\delta_v\right) \\
(J_z+\lambda_{66})\dot{r}-my_G\dot{u}+(mx_G+\lambda_{26})\dot{v}-J_{zx}\dot{p}-J_{zy}\dot{q}+J_{xy}\left(q^2-p^2\right)+\left(J_y-J_x\right)pq+mx_G(ur-wp)-my_G(wq-vr)+J_{zx}qr-J_{zy}rp \\
=\Delta Bl_b\cos\theta\cos\varphi+Gx_G\cos\theta\cos\varphi-Gy_G\sin\theta+\frac{1}{2}\rho V_B^2SL(N'_\alpha\alpha+N'_rr'+N'_{\delta h}\delta_h)
\end{cases}
\tag{8}
$$

$$
\begin{cases}
\dot{\varphi}=p-(q\cos\varphi-r\sin\varphi)\tan\theta \\
\dot{\psi}=(q\cos\varphi+r\sin\varphi)/\cos\theta \\
\dot{\theta}=q\sin\varphi+r\cos\varphi \\
\dot{\xi}_B=u\cos\theta\cos\psi+v(\sin\psi\sin\varphi+\sin\theta\cos\psi\cos\varphi)+w(\sin\psi\cos\varphi+\sin\theta\cos\psi\sin\varphi) \\
\dot{\eta}_B=u\sin\theta+v\cos\theta\cos\varphi-w\cos\theta\sin\varphi \\
\dot{\zeta}_B=-u\cos\theta\sin\psi+v(\cos\psi\sin\varphi+\sin\theta\sin\psi\cos\varphi)+w(\cos\psi\cos\varphi-\sin\theta\sin\psi\sin\varphi)
\end{cases}
\tag{9}
$$

Note that

$$
V_B=\sqrt{u^2+v^2+w^2}\ ,\ \alpha=\arctan\left(-\frac{v}{u}\right),\ \beta=\arcsin\left(\frac{w}{V_B}\right)
$$

$$
p'=\frac{pL}{V_B}\ ,\ q'=\frac{qL}{V_B}\ ,\ r'=\frac{rL}{V_B}
$$

and

$$
\begin{cases}
J_{xy}=m_rx_{Gr}y_{Gr}+m_px_{Gp}y_{Gp}+m_hx_{Gh}y_{Gh} \\
J_{yz}=m_ry_{Gr}z_{Gr}+m_py_{Gp}z_{Gp}+m_hy_{Gh}z_{Gh} \\
J_{zx}=m_rz_{Gr}x_{Gr}+m_pz_{Gp}x_{Gp}+m_hz_{Gh}x_{Gh}
\end{cases}
$$

$$
\begin{cases}
J_x=J_{xr}+J_{xp}+J_{xh} \\
J_y=J_{yr}+J_{yp}+J_{yh} \\
J_z=J_{zr}+J_{zp}+J_{zh}
\end{cases}
$$

For the vehicle, the control variables are the rotating angle of roll mass δ_r, the translational displacement of pitch mass Δl_p, the buoyancy change of bladder ΔB, the deflection angle of horizontal rudder and vertical rudder δ_h and δ_v. The definition of the variables and the range of parameter value are listed in Table I.

TABLE I
HYDRODYNAMIC AND PHYSICAL PARAMETERS

Control Var.	*Range*	*Description*
ΔB	-7~7N	Buoyancy change from external bladder
Δlp	-0.2~0.2 m	Shift displacement of pitch weight
δr	-π/2~π/2 rad	Pendulum angle for the roll weight
n	-17~17 r/s	Rotational speed of propeller
δh	-π/4~π/4 rad	Deflection angle of horizontal fins
δv	-π/4~π/4 rad	Deflection angle of vertical fins

For the specific configuration of the hybrid vehicle, the vector of mass center of roll mass, pitch mass and floating main mass should be written as

$$
\mathbf{R}_{\mathrm{r}}=\begin{bmatrix}x_{Gr}\\y_{Gr}\\z_{Gr}\end{bmatrix}=\begin{bmatrix}l_{rx}\\l_{rr}\cos\delta_r\\l_{rr}\sin\delta_r\end{bmatrix}
$$

$$
\mathbf{R}_{\mathrm{p}}=\begin{bmatrix}x_{Gp}\\y_{Gp}\\z_{Gp}\end{bmatrix}=\begin{bmatrix}l_p+\Delta l_p\\0\\0\end{bmatrix},\ \mathbf{R}_{\mathrm{m}}=\begin{bmatrix}x_{Gh}\\y_{Gh}\\z_{Gh}\end{bmatrix}=\begin{bmatrix}l_{xh}\\l_{yh}\\0\end{bmatrix}
$$

According to [19], all the physical parameters and hydrodynamic coefficients are presented in Table II and III.

TABLE II
GEOMETRIC AND PHYSICAL PARAMETERS

notation	value	unit	notation	value	unit
l_b	1.30	m	D	0.18	m
m_r	1.38	kg	J_{xGr}	0.0026	$kg\cdot m^2$
l_{rr}	0.045	m	J_{yGr}	0.0013	$kg\cdot m^2$
L_{rx}	0.63	m	J_{zGr}	0.0015	$kg\cdot m^2$
m_p	9	kg	J_{xGp}	0.0368	$kg\cdot m^2$
l_p	0.5	m	J_{yGp}	0.0496	$kg\cdot m^2$
m_h	119.18	kg	J_{zGp}	0.0497	$kg\cdot m^2$
l_{hy}	-0.02	m	J_{xGh}	1.1739	$kg\cdot m^2$
L	3.19	m	J_{yGh}	87.324	$kg\cdot m^2$
S	0.06	m^2	J_{zGh}	86.655	$kg\cdot m^2$

TABLE III
HYDRODYNAMIC COEFFICIENTS

Coef.	Value	description
λ_{11}	12 kg	Added mass
λ_{22}	170.49 kg	
λ_{33}	125.79 kg	
λ_{26}	-46 kg·m	Added moment
λ_{35}	31 kg·m	
λ_{44}	6 kg·m^2	Added moment of inertia
λ_{55}	46 kg·m^2	
λ_{66}	52 kg·m^2	
X_n'	0.21	Force coefficient along x axis
X_0'	-0.34	
K_p'	-0.2	Torque coefficient about x axis
K_n'	0.033	
Y_α'	10	Force coefficient along y axis
Y_r'	2	
$Y_{\delta h}'$	-0.68	
M_β'	0.4	Torque coefficient about y axis
M_q'	-0.145	
$M_{\delta v}'$	0.21	
Z_β'	3	Force coefficient along z axis
Z_q'	-0.58	
$Z_{\delta v}'$	0.68	
N_α'	-0.61	Torque coefficient about z axis
N_r'	-0.157	
$N_{\delta h}'$	0.21	

IV. EQUILIBRIUM AND MANEUVERABILITY

A. Equilibrium Analysis

When the vehicle is cruising in a stable state, the resultant external force and torque are all zero, then the linear and angular acceleration is all zero. For the equilibrium state in longitudinal plane, the linear and angular velocities are zero. So the equilibrium equations are deduced with (8) as

$$\begin{cases} 0 = \Delta B \sin\theta + X_n' \rho n^2 D^4 + \frac{1}{2}\rho V_B^2 S X_0' \\ 0 = \Delta B \cos\theta + \frac{1}{2}\rho V_B^2 S\left(Y_\alpha' \alpha + Y_{\delta h}' \delta_h\right) \\ 0 = \Delta B l_b \cos\theta + G x_G \cos\theta - G y_G \sin\theta + \frac{1}{2}\rho V_B^2 S L\left(N_\alpha' \alpha + N_{\delta h}' \delta_h\right) \end{cases} \tag{10}$$

By synthesizing (10), the resultant velocity, balance deflection angle of horizontal rudders and balance attack angle can be written as

$$\begin{cases} V_B = \sqrt{\dfrac{2\left(\Delta B \sin\theta + X_n' \rho n^2 D^4\right)}{-\rho S X_0'}} \\ \overline{\alpha} = \dfrac{-2\Delta B \cos\theta}{\rho V_B^2 S Y_\alpha'} - \dfrac{Y_{\delta h}' \delta_h}{Y_\alpha'} \\ \overline{\delta}_h = \dfrac{2\Delta B \cos\theta\left(L N_\alpha' - l_b Y_\alpha'\right) + 2 G Y_\alpha'\left(y_G \sin\theta - x_G \cos\theta\right)}{\rho V_B^2 S L\left(Y_\alpha' N_{\delta h}' - N_\alpha' Y_{\delta h}'\right)} \end{cases} \tag{11}$$

From (11), the resultant velocity is determined both by the thrust force and controllable buoyancy of external bladder. The balance angle of horizontal rudder is determined both by the internal mass redistribution and buoyancy change. The balance attack angle is associated with rudder angle and buoyancy change.

The stable glide operation in the longitudinal plane can be accomplished by setting δ_h=0, δ_r=0 and n=0, and tuning ΔB and Δl_p. During the glide process, the balance attack angle becomes

$$\overline{\alpha}_g = \frac{-2\Delta B \cos\theta}{\rho V_B^2 S Y_\alpha'}$$

The gravity center is depicted as

$$\begin{cases} x_G = \dfrac{m_r l_{rx} + m_p (l_p + \Delta l_p) + m_h l_{xh}}{m} \\ y_G = \dfrac{m_r l_{rr} \cos\delta_r + m_h l_{yh}}{m} \end{cases}$$

Substitute the expressions of balance attack angle and gravity center above into (10), the equation of balance pitch angle in glide operation yields

$$\tan\overline{\theta}_g = \frac{\Delta B m\left(Y_\alpha' l_b - L N_\alpha'\right) + G m_p \Delta l_p Y_\alpha' + G Y_\alpha'\left(m_r l_{rx} + m_p l_p + m_h l_{xh}\right)}{G Y_\alpha'\left(m_r l_{rr} + m_h l_{yh}\right)} \tag{12}$$

According to (12) we know that the pitch angle can be determined both by buoyancy change and pitch mass. It is energy efficient to place the buoyancy bladder in the nose section of vehicle, in that the buoyancy change does contribution to pitch moment and then shortens the displacement of pitch mass.

During stable thrust operation, the balance pitch angle can be regulated by internal mass and the horizontal rudder. By substituting ΔB=0 into (11), the balance attack angle in thrust mode yields

$$\overline{\alpha}_t = -\frac{Y_{\delta h}' \delta_h}{Y_\alpha'}$$

By synthesizing balance attack angle with (10), we get

$$\sin\left(\overline{\theta}_t - \gamma\right) = \frac{c}{\sqrt{a^2 + b^2}} \quad \tan\gamma = \frac{b}{a}$$

By rearranging, the stable pitch angle is calculated as

$$\overline{\theta}_t = \arcsin\frac{c}{\sqrt{a^2 + b^2}} + \arctan\frac{b}{a} \tag{13}$$

where

$$\begin{cases} a = 2GY'_{\alpha}\left(m_r l_{rr} + m_h l_{yh}\right) \\ b = 2GY'_{\alpha} m_p \Delta l_p + 2GY'_{\alpha}\left(m_r l_{rx} + m_p l_p + m_h l_{xh}\right) \\ c = m\rho V_B^2 SL\delta_h\left(Y'_{\alpha}N'_{\delta h} - N'_{\alpha}Y'_{\delta h}\right) \end{cases}$$

From the (13), while the vehicle is navigating at low speed or even stopping, the pitch attitude is hard to keep only with the horizontal rudder, whereas the pitch mass can take part in the regulating of pitch attitude.

B. *Maneuverability investigation*

According to [20], maneuverability shows the ability for the control forces to generate the acceleration of motion of vehicle, i.e. the ability to change the direction and magnitude of the velocity vector. The overload vectors and swerving radius is often used to indicate the maneuverability.

Generally, conventional AUVs will be in bad condition to maneuver at low speed, but legacy glider performs attitude control very well even when remaining stationary in water. Conventional AUVs use the hydrodynamic of rudders to change its attitude however legacy gliders utilize the internal mass redistribution to change its orientation. Due to the difference of motion modes and driving principles, the expressions of the maneuverability of conventional AUVs, legacy gliders and hybrid vehicles is not the same too. In order to illustrate the maneuverability of hybrid class gliders, a set of more comprehensible index formula should be deduced.

The hybrid glider PETREL is redundant actuated system, and can perform 6-DOF of control of position and attitude. The expressions of maneuverability are divided into 6 types corresponding to the 6 degrees of freedom: surge, heave, sway, roll, yaw and pitch. The maneuverability of surge, heave and sway is evaluated with the control force, damping force and total mass, and the corresponding equations are defined as

The surge maneuverability:

$$f_{\dot{u}} = \frac{\left(X'_n \rho n^2 D^4 + \Delta B \sin\theta\right) + \frac{1}{2}\rho V_B^2 S X'_0}{m + \lambda_{11}} \tag{14}$$

The heave maneuverability:

$$f_{\dot{v}} = \frac{\left[\Delta B\cos\theta + \frac{1}{2}\rho V_B^2 S\left(Y'_{\alpha}\alpha + Y'_{\delta h}\delta_h\right)\right] + \frac{1}{2}\rho V_B^2 S Y'_r r'}{m + \lambda_{22}} \tag{15}$$

The sway maneuverability:

$$f_{\dot{w}} = \frac{\frac{1}{2}\rho V_B^2 S\left(Z'_{\beta}\beta + Z'_{\delta v}\delta_v\right) + \frac{1}{2}\rho V_B^2 S Z'_q q'}{m + \lambda_{33}} \tag{16}$$

The maneuverability of roll, yaw and pitch is calculated with driving torque, damping moment and moment of inertia, and the corresponding expressions are written as

The roll maneuverability:

$$f_{\dot{p}} = \frac{\left[K'_n \rho n^2 D^5 - G\left(z_G\cos\varphi + y_G\sin\varphi\right)\right] + \frac{1}{2}\rho V_B^2 SLK'_p p'}{J_x + \lambda_{44}} \tag{17}$$

The yaw maneuverability:

$$f_{\dot{q}} = \frac{\frac{1}{2}\rho V_B^2 SL\left(M'_{\beta}\beta + M'_{\delta v}\delta_v\right) + \frac{1}{2}\rho V_B^2 SLM'_q q'}{J_y + \lambda_{55}} \tag{18}$$

The pitch maneuverability:

$$f_{\dot{r}} = \frac{\begin{bmatrix} \Delta B l_b\cos\theta + \left(Gx_G\cos\theta - Gy_G\sin\theta\right) \\ + \frac{1}{2}\rho V_B^2 SL\left(N'_{\alpha}\alpha + N'_{\delta h}\delta_h\right) \end{bmatrix} + \frac{1}{2}\rho V_B^2 SLN'_r r'}{J_z + \lambda_{66}} \tag{19}$$

Note that the first items in numerators of equations of maneuverability are the active control force/torque and increase the maneuverability while the second items counteract the first items as a drag force/moment. The approach to improve the maneuverability is to increase the control quantum, decrease the damping force/moment and mass/moment of inertial.

C. *Effect of fixed wings on vehicle*

The hybrid-driven underwater glider can be simplified as an autonomous underwater vehicle (AUV) mounted with fixed wings while operated in thrust mode. To investigate the impact of fixed wings on the performance of PETREL, hydrodynamic experiment and simulation was conducted to derive the hydrodynamic parameters of vehicle with fixed wings and no wings. Results show that the fixed wings considerably enlarge the hydrodynamic lift and have little impact on the other hydrodynamic coefficients.

Equation (15) is reduced by setting the buoyancy change and the displacement of internal mass to be 0. The maneuverability in longitudinal plane is obvious by changing the sensitive hydrodynamic coefficients. Fixed wings increase the hydrodynamic lift of AUV and simultaneously enhance its maneuverability in the longitudinal plane.

Without loss of generality, we keep the other parameters the same and only change the hydrodynamic lift coefficients. Y'_{α}=11 indicates the vehicle is mounted with fixed wings, whereas Y'_{α}=4 indicates the vehicle is without wings. By setting the initial surge and heave velocity as 0.01 and 0, assigning ΔB=0, Δl_p=0, δ_r=0, n=800r/min, δ_v=0, and giving varied values of deflection angles of horizontal rudders, the simulation is performed.

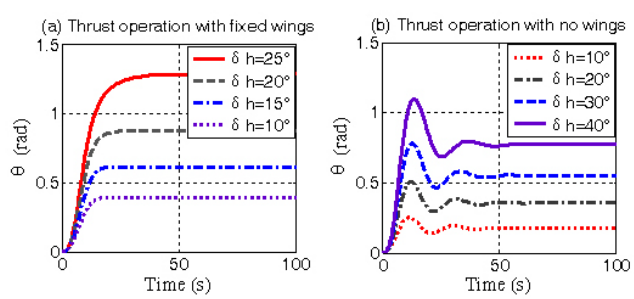

Figure 4. Capability of pitch control with horizontal rudders.

The response characteristic of pitch attitude is illustrated in Fig.4. It is indicated that the attitude control capability with deflectable rudders is largely improved and the overshoot and oscillation are eliminated while using fixed wings. Regardless of the little drag increased, adding fixed wings to AUV substantively improves the maneuverability and the stability.

That's to say, the existence of fixed wings seems to add a pivot to the middle of vehicle and facilitate pitch control for the horizontal rudders without lost the longitudinal stability while the hybrid vehicle navigates in thrust mode.

D. Contrast of turning capability

The hybrid glider PETREL changes direction of motion in glide operation by rotating the roll mass or/and deflecting the horizontal rudders. For the contrast of the capability of swerving, we do the simulation of helix glide motion.

Set the rotating angle of roll mass δ_r as the maximum value 1.57rad. Select the simulation time 2000 seconds and the initial velocity 0.001m/s. The values of other control variables are assigned as: buoyancy change 7N, displacement of pitch mass -0.1m, speed of prop 0r/s, deflection angles of horizontal and vertical rudders 0 rad.

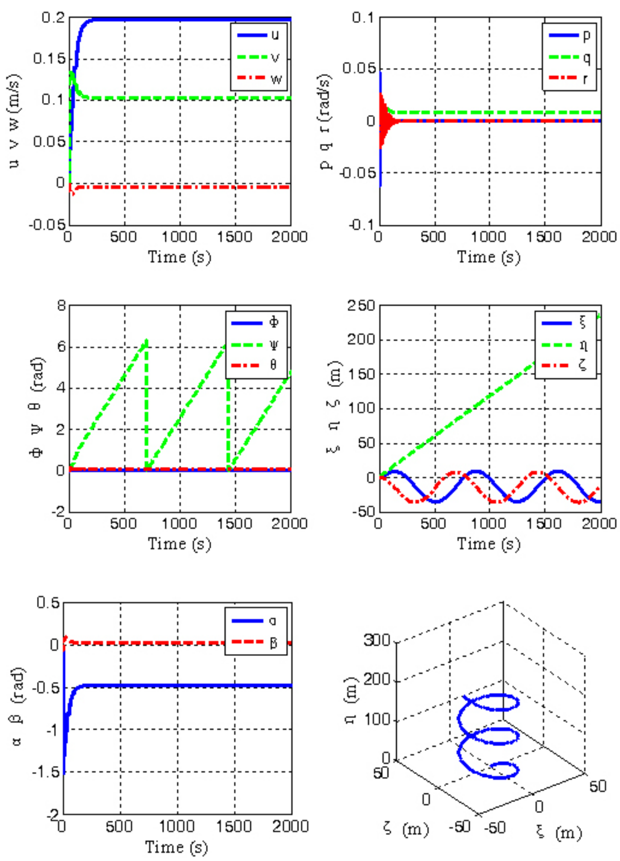

Figure 5. Helix glide motion with roll mass for steering.

As shown in Fig. 5, the motion takes 370 seconds to perform a circle. The turning diameter and the thread pitch are respectively 44.3 meters and 43.2 meters. During the stable glide, u=0.197m/s, v=0.102m/s, w=-0.005m/s, q=0.0085rad/s, a=-0.4793rad, b= -0.0213rad.

Set the deflection angle of vertical rudders as the maximum value 0.7 rad. Select the simulation time 1000 seconds and initial velocity 0.001m/s. The values of other control variables are assigned as: buoyancy change 7N, displacement of pitch mass -0.1m, speed of prop 0r/s, deflection angle of horizontal 0rad, the rotating angle of roll mass 0rad.

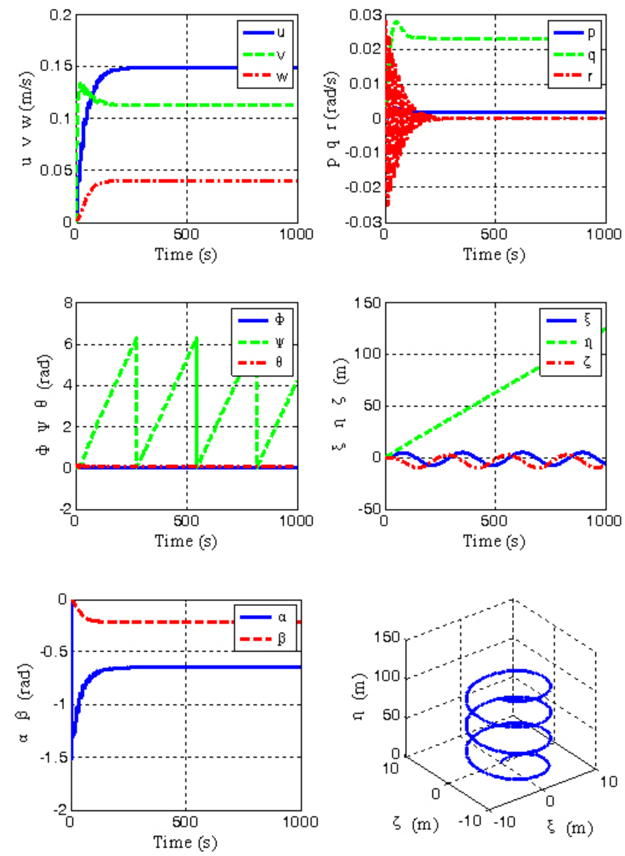

Figure 6. Helix glide motion with vertical rudders for steering.

As shown in Fig. 6, the motion takes 136 seconds to perform a circle. The turning diameter and the thread pitch are respectively 12.5 meters and 16.8 meters. During the stable glide, u=0.15m/s, v=0.11m/s, w=0.04m/s, q=0.023rad/s, a=-0.648rad, b= -0.2127rad.

From the above analysis, the maximum swerving capability of PETREL is more remarkable by deflecting the vertical rudder for steering than by rotating the roll mass.

V. Field Trial Analysis

Lake trials were conducted successively and the fundamental performance was testified. Profiling experiment was tested in Fuxian Lake, China, July 2009. In this test, pitch vernier mechanism shifts internal mass forward and backward to coordinate the decrement and increment of buoyancy. The dive depth is set to be -20 meters, the displacement of pitch mass is +-0.15m, and the volume change of external bladder is +-500cc. The deflection angles of rudders were all reset to

0 and the prop did not rotate. As shown in Fig. 7 is the profiling curves in this glide operation. The hybrid PETREL takes 120 seconds to arrive at the preprogrammed depth -20m, the descending/ascending velocity can be rated as 0.18 m/s by taking the process of the acceleration into consideration, the balance pitch angle is +-33 degrees in the surfacing/diving operation. The sampling period is 1 second.

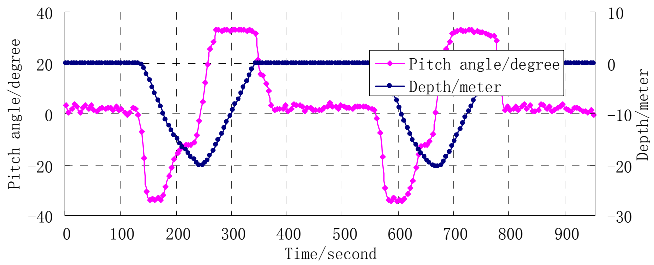

Figure 7. Profiling in glide operation

Fixed depth navigating experiment were also performed in Fuxian Lake, July 2009. In this test, PETREL controlled the deflection angle of horizontal rudders and maintained the predetermined depth of -15m with a proceeding velocity 1m/s. Pitch vernier mechanism shifts internal mass (li-ion battery pack) forward to help vehicle nose down when begins a fixed depth navigating. As shown in Fig.8 is the recorded curves in thrust operation. The sampling period is 1 second.

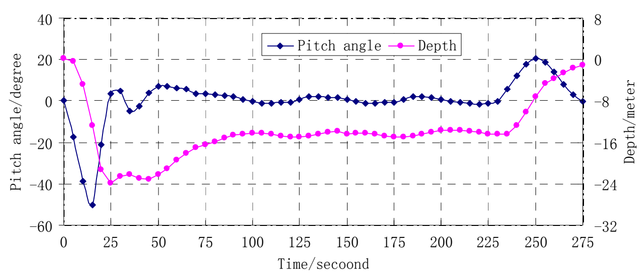

Figure 8. Fixed depth cruising in thrust operation.

The navigation experiment and swerving test were conducted in Youth Pool, Tianjin University from March to July (Fig.9). Swerve test aims to test the cruising diameter in case of a variety of deflection angles of vertical rudders. In the swerving test, one single vertical rudder immersed in water, the deflection angle of vertical rudders were set as 30 degrees, and the prop rotated at a speed of 500r/m, this vehicle will accomplish a circular voyage with a diameter of 40 meters. Navigation trial aims to test the ability to follow the prescribed path. According to GPS fix, PETREL corrects its direction by deflecting vertical rudders every second. The vehicle was launched from A point and tracks the preset path to arrive at B point for recovery.

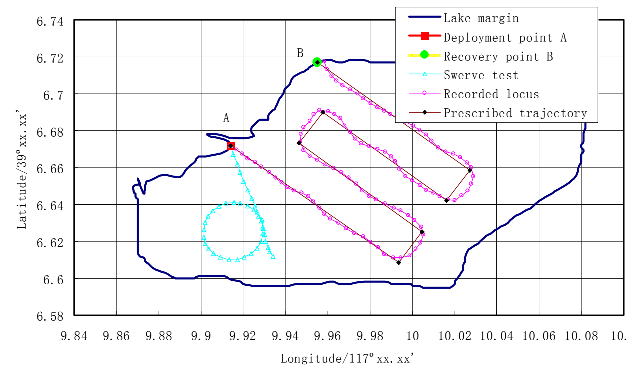

Figure 9. Navigation experiment in thrust operation.

VI. Conclusions

PETREL is the latest in the lineage of hybrid-driven underwater gliders developed and is being constructed and tested at Tianjin University. PETREL, the winged hybrid-driven underwater glider combines functions of legacy gliders and conventional AUVs. By changing propulsion methods to suite local conditions, PETREL can use the best aspects of both an AUV and an underwater glider without being hampered by the drawbacks of each. This hybrid vehicle can overcome the disadvantages such as deficiency in maneuverability for present gliders and high power consumption for AUVs etc.

In addition, the dynamic model is constructed by tailoring the theorem of momentum to the particular configuration of PETREL, and the equilibrium and maneuverability equations are deduced for the evaluation of the performance of the hybrid. According to the theory analysis and computer simulation, the conclusions are as follows:

1. In glide operation, the external bladder for buoyancy change improves the efficiency of pitch control while mounted on the fore end of vehicle and the swerving radius is largely decreased by using vertical fins for steering instead of roll mass;

2. In thrust operation, the longitudinal maneuverability is largely increased due to the fixed wings and the capability of attitude keeping is augmented by redistribution of internal mass (roll and pitch mass) while the vehicle cruises at low speed.

During several months of field trial, the parts of experiment data was obtained, and the fundamental functions were validated. This practice shows that the effort to fabricate the PETREL is meaningful. In the later days, we aim to improve its robust control capability and reliable manipulation ability.

Acknowledgment

This work is supported by National Natural Science Foundation of China (No. 50835006 and No. 50705063). The authors appreciate all staff members in this research and development team.

REFERENCES

[1] D.L. Rudnick, R.E. Davis, C.C. Eriksen, "Underwater Glider for Ocean Research," *Marine Technology Society Journal,* vol. 38(1), pp. 48-59, Spring 2004.

[2] K.M. Tan, T. Liddy, A. Anvar, T.F. Lu, "The advancement of an autonomous underwater vehicle (AUV) technology," *IEEE Conference on Industrial Electronics and Applications*, pp. 336-341, 2008.

[3] J.G. Wu, C.Y. Chen, S.X. Wang, "Hydrodynamic Effects of a Shroud Design For a Hybrid-Driven Underwater Glider," *Sea Technology*, December 2009, In Press.

[4] J. Sherman, R.E. Davis, W.B. Owens, and J. Valdes, "The Autonomous Underwater Glider 'Spray'," *IEEE Journal of Oceanic Engineering,* vol. 26(4), pp. 437-446, October 2001.

[5] D.C. Webb, P.J. Simonetti, and C.P. Jones, "SLOCUM: An Underwater Glider Propelled by Environmental Energy," *IEEE Journal of Oceanic Engineering,* vol. 26(4), October 2001.

[6] T.J. Osse, R.D. Light, T. Wen, T.W. Lehman, "Seaglider: A Long-range Autonomous Underwater Vehicle for Oceanographic Research," *IEEE Journal of Oceanic Engineering,* vol. 26(4), pp. 424-436, October 2001.

[7] J.R. Perrett, M. Pebody, "Autosub-1. Implications of Using Distributed System Architectures in AUV Development," *IEEE Conference Publication*, n. 439, pp. 9-15, 1997.

[8] R. Alexander, V.A. Chris, A. Ben, F. Ned, "Development of the REMUS 600 Autonomous Underwater Vehicle," *Proceedings of MTS/IEEE OCEANS*, 2005.

[9] Y. Richard, "Surveying the Underside of an Arctic Ice Ridge Using a Man-portable GAVIA AUV Deployed through the Ice," Oceans 2007 MTS/IEEE Conference, 2007.

[10] S. Araki, K. Ishii, "Development of glider type small AUV 'SeaBird'," *International Symposium on Underwater Technology*, pp. 320-325, 2007.

[11] R. Bachmayer, N.E. Leonard, J. Graver, E. Fiorelli, P. Bhatta and D. Paley, "Underwater Gliders: Recent Developments and Future Applications," *Proceedings of the 2004 International Symposium on Underwater Technology,* pp. 195-200, 2004.

[12] S. Wood, T. Allen, S. Kuhn, J. Caldwell, "The Development of an Autonomous Underwater Powered Glider for Deep-Sea Biological, Chemical and Physical Oceanography," *OCEANS 2007-Europe,* 2007.

[13] A. Caffaz, A. Caiti, G. Casalino, L. Gualdesi, "Fòlaga: A Low-cost Autonomous Underwater Vehicle Combining Glider and AUV Capabilities," *Ocean Engineering*, vol. 36(1), pp. 24-38, January 2009.

[14] G. Griffiths, C.P. Jones, J. Ferguson, N. Bose, "Undersea Gliders," *Journal of Ocean Technology*, 2007.

[15] D.R. Blidberg, "The Development of Autonomous Underwater Vehicles; a Brief Summary," *IEEE International Conference on Robotics and Automation*, Korea, pp. 1-12, 2001.

[16] T.S. Li, Torpedo Maneuverability, National Defense Industry Press, 1999.

[17] Y.H. Wang, S.X. Wang. "Dynamic Modeling and Three-dimensional Motion Analysis of Underwater Gliders," *China Ocean Engineering*, vol. 23(3), pp. 489-504, September 2009.

[18] X.M. Wang, *Dynamical Behavior and Control Strategies of the Hybrid Autonomous Underwater Vehicle*, Ph. D. Thesis, Tianjin University, 2009.

[19] J.G. Wu, *System Design and Performance Analysis of Hybrid-Driven Underwater Glider*, Ph. D. Thesis, Tianjin University, 2010.

[20] J.D. Song, Analysis and Design of Performance of Underwater Launched Capsules, Beijing: National Defense Industry Press, 2008.